

Effects of Doping on Electronic Structure and Correlations in Carbon Peapods

Ling Ge,^{†,*} John H. Jefferson,[‡] Barbara Montanari,[§] Nicholas M. Harrison,[⊥] David G. Pettifor,[†] and G. Andrew D. Briggs[†]

[†]Department of Materials, University of Oxford, Oxford OX1 3PH, United Kingdom, [‡]Sensors and Electronics Division, QinetiQ, St Andrews Road, Malvern, Worcs. WR14 3PS, United Kingdom, [§]STFC Rutherford Appleton Laboratory, Didcot, Oxfordshire OX11 0QX, United Kingdom, and [⊥]Department of Chemistry, Imperial College, London SW7 2AZ, United Kingdom

Doping *via* donors or acceptors is a critical technique for many electronic applications of carbon nanotubes.^{1,2} Semiconducting or metallic single-wall carbon nanotubes (SWNTs) can be filled with fullerenes, forming the so-called carbon peapods, to modify and control their electronic properties at the nanoscale.³ The fabrication of nanoscale electronic devices such as field effect transistors (FETs) with carbon peapods containing various fullerenes or endohedral fullerenes is well established.⁴ Electronic transport measurements (*i.e.*, the drain current as a function of the gate biases) of FETs with several types of peapod such as SWNTs containing C₆₀, C₇₈, C₉₀, La@C₈₂, Gd@C₈₂, Dy@C₈₂, La₂@C₈₀, Ti₂@C₈₀, Ce₂@C₈₀ and Gd₂@C₉₂ fullerenes have been reported.^{5–10} These results show that the band gap of the peapods depends on (1) the insertion of fullerenes or metallofullerenes, (2) the intrafullerene charge transfer, that is, from the metal atom to the carbon cage, and (3) the size of the encapsulated fullerenes. Theoretical calculations are needed to establish the mechanisms underpinning these observed correlations, such as the charge transfer mechanism, the effects of doping on the electronic structure and correlations in carbon peapods, and the possible conductive pathways in the above experimental measurements.

Previous theoretical studies using hybrid density functional theory (DFT) on SWNTs containing Sc@C₈₂ reveal that the bands derived from the highest occupied molecular orbital (HOMO) and the lowest unoccupied molecular orbital (LUMO) of Sc@C₈₂ are separated by an energy gap of 0.530 eV. We denote the two fullerene bands as the upper and lower Hubbard

ABSTRACT Sc@C₈₂ peapods, which form encapsulated spin-1/2 antiferromagnetic chains under doping with electrons or holes are investigated using hybrid density functional theory. The narrow fullerene bands become shifted relative to nanotube bands resulting in charge transfer and conducting channels along both the fullerene chain and the nanotube. This is accompanied by a reduction in the magnetic moments on the fullerenes, consistent with a 1D Hubbard—Anderson model description.

KEYWORDS: doping · electronic structure · fullerenes · nanotubes · conducting channels · correlated electron models · spintronics

bands. Remarkably, the upper and lower Hubbard bands of the fullerene chain lie entirely within the band gap of the semiconducting (14,7) SWNT, and the system is a Mott insulator.¹¹

In this paper we investigate the effects of doping of peapods away from the Mott insulating regime of the Sc@C₈₂ chain within the nanotube, which is potentially significant in several respects. First, this is relevant to transistor-like devices or other gated structures in which there is charge transfer to and from the peapod. Second, we expect this to be a highly correlated conductor and the question arises as to where the mobile charge resides. If it remains on the fullerene chain then this will essentially become a one-dimensional doped Mott insulator, encased in either a semiconducting or metallic nanotube. Conversely, if there is charge transfer to the nanotube then there will always be two parallel one-dimensional conducting channels, expected to be weakly interacting; a weakly correlated conductor along the nanotube and a strongly correlated conductor along the encapsulated chain. To investigate these possibilities we have performed calculations of Sc@C₈₂ chains and peapod structures with both semiconducting and metallic nanotubes and doping levels in

*Address correspondence to ling.ge@materials.ox.ac.uk.

Received for review December 9, 2008 and accepted April 01, 2009.

Published online April 7, 2009.
10.1021/nn8008454 CCC: \$40.75

© 2009 American Chemical Society

which an average of either 1/2 or 1 electron per fullerene is added or subtracted.

First, we give details of the computational method used. This is followed by an analysis of a Sc@C₈₂ chain in which the fullerenes are separated by the same distance they have when encapsulated in the (14,7) peapod. We also compare the DFT results with a mean-field treatment of a simplified Hubbard model and demonstrate their consistency, extracting hopping, and Coulomb repulsion parameters. Then the results of DFT simulations of peapod structures with both semiconducting and metallic nanotubes are presented and the charge rearrangement between fullerene chain and nanotubes is determined. We show how these results are consistent with an extended Hubbard–Anderson model for two weakly interacting conduction channels on the chain and the nanotube. Finally we summarize the main results and conclusions.

RESULTS AND DISCUSSION

We have performed total-energy band-structure DFT calculations of electron or hole-doped Sc@C₈₂ fullerene chains and peapods with the hybrid exchange density functional B3LYP^{12–14} as implemented in the CRYSTAL package.¹⁵ The calculations reported here are all-electron, that is, with no shape approximation to the ionic potential or electron charge density. The geometry optimizations are performed using the algorithm proposed by Schlegel *et al.*¹⁶ The crystalline wave functions are expanded in Gaussian basis sets of double valence quality (6-21G* for carbon and 864-11G* for scandium). Atomic charges are estimated using Mulliken population analysis.¹⁷ The system is modeled as a three dimensionally periodic array with reciprocal space sampling performed on a Monkhorst–Pack grid containing 30 symmetry irreducible *k*-points which converges the total energy to within 10^{−4} eV per unit cell. The center-to-center distance between the tubes in neighboring tetragonal unit cell is 30 Å, large enough to eliminate direct tube–tube interactions. As model systems, we choose Sc@C₈₂ in (14,7) (semiconducting) and (11,11) (metallic) SWNTs. Our calculations predict an exothermic encapsulation of Sc@C₈₂ for both tubes. The repeat units containing one Sc@C₈₂ molecule in the (14,7) and (11,11) peapods are 11.42 and 12.47 Å, respectively.¹⁸ The interwall separations between the (14,7) and (11,11) tubes and Sc@C₈₂ are 3.35 Å (van der Waals distance) and 3.55 Å, respectively. The relaxed structure of an isolated Sc@C₈₂ molecule is found to be in agreement with ref 19 with a Sc–C distance of 2.26 Å. The doping levels considered are one electron or hole per unit cell containing one Sc@C₈₂ fullerene in (14,7) and (11,11) tubes, or one electron per unit cell containing two Sc@C₈₂ fullerenes in the same tubes, with a uniform charged background of opposite sign to neutralize the system. For charged Sc@C₈₂ chain and peapods,

the results are obtained at the optimized geometries for the corresponding neutral systems.

First we will present the results of doped Sc@C₈₂ chains which are stepping stones for an understanding of the more complicated peapods systems. Figure 1 shows the electronic structures of neutral and charged Sc@C₈₂ chains. Figure 1a shows a chain of parallel spins, which we denote as the ferromagnetic (FM) state. The state is found to be a Mott insulator with a band gap of 0.530 eV. The fullerene band derived from the HOMO of Sc@C₈₂ splits into an occupied and an unoccupied band. For a chain of Sc@C₈₂ molecules doped with one electron per fullerene, the electronic structures of spin-up and spin-down electrons are identical. The unpaired electron of Sc@C₈₂ and the additional electron occupy one spin-up orbital and one spin-down orbital giving a filled-band insulator. Figure 1c or 1d shows a chain of Sc@C₈₂ doped with 1/2 electron or hole per fullerene, respectively; the unit cell contains two fullerenes. The Fermi energy is where the bands touch at the zone boundary which is consistent with a half-filled conduction band for the extended zone with one fullerene per unit cell. In both cases, the unpaired electron is shared equally between two fullerenes in the unit cell. At the Γ point, the unpaired electron is in a bonding orbital, and the lowest unoccupied band is in an antibonding orbital. The energy gap between bands in spin-up and spin-down derived from the HOMO is 0.270 eV.

It has been shown that a Hubbard model with the hopping parameter, $t = 0.017$ eV for the interfullerene spacing $R = 11.42$ Å (cage center-center distance), and the intrafullerene Coulomb repulsion, $U = 0.530$ eV, is a good approximation to the electronic structure of undoped peapods.¹¹ Here it can be used to gain insight into the effects of doping. The Hamiltonian is

$$H_{fc} = \sum_{k\sigma} E_{k\sigma} a_{k\sigma}^\dagger a_{k\sigma} + U \sum_i n_{i\uparrow} n_{i\downarrow} \quad (1)$$

where E_k are the dispersion energies of the bands derived from the HOMO of Sc@C₈₂ with quasi-momentum k , $a_{k\sigma}^\dagger$ is a creation operator for an electron in the HOMO-derived band of the fullerenes with spin σ , U is the intrafullerene Coulomb repulsion energy, and $n_{i\sigma} = a_{i\sigma}^\dagger a_{i\sigma}$ is the number operator for an electron of spin σ in the HOMO-derived Wannier function on the i th fullerene.

When the Hubbard– U term is treated in mean-field theory, the Hamiltonian (1) reduces to the one-electron form,

$$\tilde{H}_{fc} = \sum_{k\sigma} E_{k\sigma} a_{k\sigma}^\dagger a_{k\sigma} \quad (2)$$

with band energies

$$E_{k\sigma} = \varepsilon_\sigma - 2t \cos k \quad (3)$$

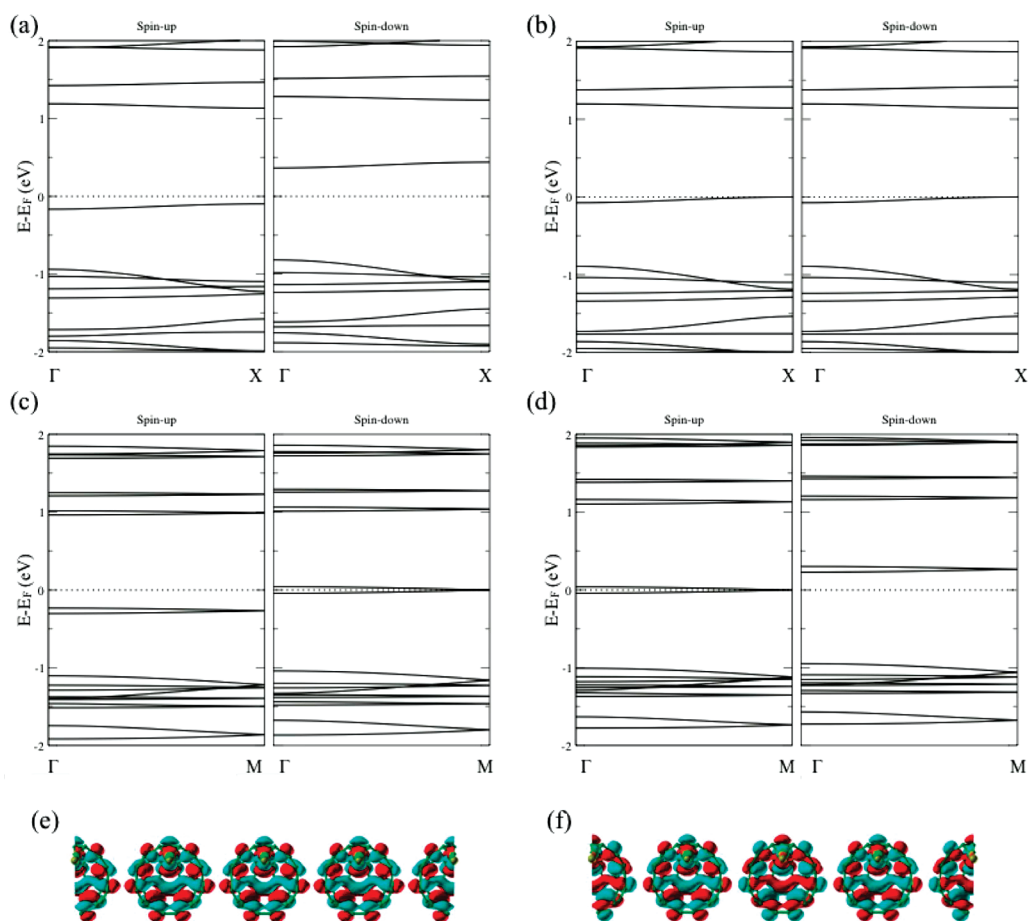


Figure 1. Spin-polarized band structures of (a) Sc@C_{82} chain for the FM configuration, (b) Sc@C_{82} chain with one extra electron per cell containing one fullerene, (c or d) Sc@C_{82} chain with $1/2$ electron or hole per fullerene, respectively; the unit cell contains two fullerenes. Left (right)-hand side refers to spin-up (-down) electrons. E_F is the Fermi energy. (e) Wave function plot of unpaired electron of $(\text{Sc@C}_{82})_2^-$ or $(\text{Sc@C}_{82})_2^+$ chain at Γ point. (f) Wave function plot of lowest unoccupied band of $(\text{Sc@C}_{82})_2^-$ or $(\text{Sc@C}_{82})_2^+$ chain at Γ point. The red and blue lobes represent positive and negative phases, respectively.

and spin-dependent on-site energies

$$\varepsilon_\sigma = \varepsilon_0 + U\langle n_{-\sigma} \rangle, \quad (4)$$

where ε_0 is the energy of a single electron in the HOMO of a fullerene and $\langle n_{-\sigma} \rangle$ is the probability of finding an electron of opposite spin on the same fullerene. Note that the energy separation of the band centers is

$$\Delta = \varepsilon_i - \varepsilon_j = U(\langle n_i \rangle - \langle n_j \rangle) = Um \quad (5)$$

where m is the mean magnetic moment. The dispersions of the HOMO and LUMO derived bands of Sc@C_{82} for the cases shown in Figure 1 show excellent fits with the cosine form of eq 3. Further consistency with the simple Hubbard model picture is given by comparing t and U for the undoped and doped cases. These results are listed in Table 1, showing excellent transferability of the model parameters. We will then discuss the validity of the Hubbard model for the chain in doped peapod systems for which there is electron transfer to the nanotube.

In the following, we discuss how the picture changes in the peapods and extend the Hamiltonian (1) to a generic Hubbard–Anderson model when the band occupancy is changed to include the nanotube bands and the interaction between fullerenes and the nanotube after doping.

Figure 2 shows the electronic charge rearrangement of an extra electron added per unit cell in the $\text{Sc@C}_{82}@(14,7)$ peapod: 40% of the charge density associated with the additional electron resides on the fullerene and 60% on the tube. Similar quantitative results are obtained for the case of removing an electron. Table 2 shows the Mulliken charge and spin populations, the energy gap Δ between the bands derived

TABLE 1. $\langle n_\uparrow \rangle$, $\langle n_\downarrow \rangle$, U , and t for Sc@C_{82} , Sc@C_{82}^- , $\text{Sc@C}_{82}^{0.5-}$, $\text{Sc@C}_{82}^{0.5+}$ Chains

system	$\langle n_\uparrow \rangle$	$\langle n_\downarrow \rangle$	U (eV)	t (eV)
Sc@C_{82}	1	0	0.530	0.017
Sc@C_{82}^-	1	1	0.530	0.018
$\text{Sc@C}_{82}^{0.5-}$	1	$1/2$	0.536	0.020
$\text{Sc@C}_{82}^{0.5+}$	$1/2$	0	0.530	0.019

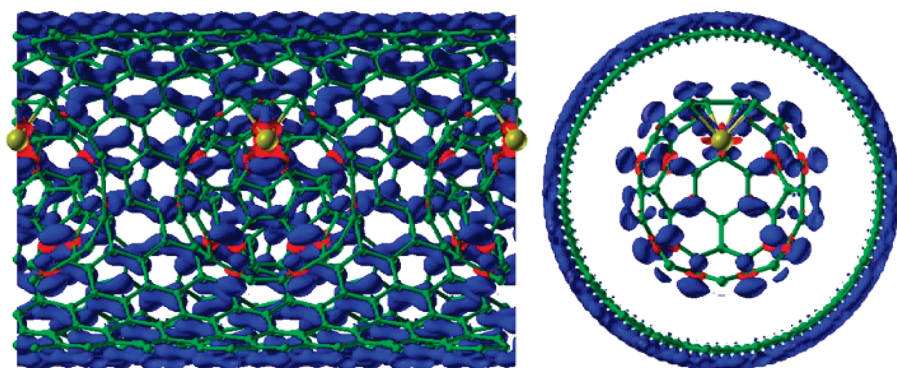


Figure 2. Difference in charge density of $\text{Sc@C}_{82}@(14,7)$ peapod with and without one extra electron per cell, which is the plot of $\rho[\text{Sc@C}_{82}@(14,7)^-] - \rho[\text{Sc@C}_{82}@(14,7)]$. Value for the blue surface is $-0.001 \text{ e}/\text{\AA}^3$. Left (right) hand shows front (side) view. The atom colored in gold is Sc.

from the HOMO and LUMO of Sc@C_{82} , in neutral $\text{Sc@C}_{82}@(14,7)$ and $\text{Sc@C}_{82}@(11,11)$ peapods, and the same systems with an added electron or hole per unit cell. In both peapods, the extra electron or hole is distributed partially on the nanotube and partially on the fullerene. The local magnetic moment on the fullerenes is reduced in charged peapods with a corresponding reduction of the energy gaps between the bands derived from the HOMO and LUMO of Sc@C_{82} , consistent with eq 5. Doping suppresses the total spin in the metallic peapod less than in the semiconducting case, consistent with a mean moment $m = \mu_B(1 - n)$, where n is the extra charge (electron or hole) residing on a fullerene.

Figure 3 shows the spin-polarized band structures of neutral and charged $\text{Sc@C}_{82}@(14,7)$ and $\text{Sc@C}_{82}@(11,11)$. Figure 3 panels a and d show the FM state, which is the configuration of the peapods with parallel spins along the Sc@C_{82} chain. The semiconducting case (Figure 3a) is a Mott insulator with Mott–Hubbard gap $\approx 0.530 \text{ eV}$ and hopping $t = 0.017 \text{ eV}$, estimated directly from the separation and dispersion of the narrow cosine bands (cf. equation 3 and 4 with $\langle n_{\uparrow} \rangle = 1$, $\langle n_{\downarrow} \rangle = 0$), consistent with weak hopping of electrons along the fullerene chain. In the metallic nanotube case (Figure 3d), these bands cross

the wide nanotube bands opening up small hybridization gaps.

Figure 3b shows the band structure of $\text{Sc@C}_{82}@(14,7)$ with one extra electron per cell. The fullerene-derived bands become shifted to higher energies relative to the undoped case causing both the LUMO-derived spin-down band and the nanotube conduction bands to become partially occupied. The fullerene chain, which is now conducting, behaves as a doped Mott insulator. Comparing Figure 3 panels a and b, the energy

gap between the top of the nanotube valence bands and the bottom of the nanotube conduction bands at the Γ point remains unchanged. Table 3 shows the shift of the spin-up and spin-down bands derived from the HOMO of Sc@C_{82} in doped peapods compared with undoped peapods. The spin-up (-down) fullerene band has been shifted upward by 0.438 (0.196) eV relative to the top of the nanotube valence bands from Figure 3a,b. This is consistent with eq 4, with $\langle n_{\uparrow} \rangle$ unchanged with doping and $\langle n_{\downarrow} \rangle$ increasing from zero. The upward shift of the fullerene bands implies that the electrons on the fullerene chain have higher energy than the electrons on the nanotube. This can be understood with a simple electrostatic model, in which we treat the fullerene chain and the nanotube as two cylindrical surfaces with different surface charge densities. A test electron between the cylinders will feel the repulsion of the electrons on the inner cylinder with potential energy decreasing like $\lambda \ln r$ where λ is the charge per unit length and r is the radial distance. On the other hand, it is a consequence of Gauss' Law that electrons on the outer tube will not affect the test electron between the tubes. Hence the potential energy of electrons on the outer tube will always be lower. This is consistent with the relative shifts of fullerene and nanotube bands shown in Figure 3 and, furthermore, explains why the effect is greater for the semiconducting tube case as the charge on the fullerenes is greater. A similar argument applies for hole doping. The energy gap between centers of the bands derived from the HOMO and LUMO of Sc@C_{82} , Δ , is 0.317 eV for $\text{Sc@C}_{82}@(14,7)$ with one extra electron per cell. This is in good agreement with eq 5, using $m = 0.6 \mu_B$ from Table 2 and $U = 0.530 \text{ eV}$. We note that the relative displacement of the nanotube and fullerene bands respect electron–hole symmetry, by which we mean that the fullerene states undergo a comparable downshift relative to the nanotube states under hole doping, as plotted in Figure 3c. Using the same reference point, the spin-up and -down fullerene levels have been shifted downward by 0.245 and 0.487 eV, respectively, compared to Figure 3a. This is again consistent with eq 4,

TABLE 2. Charge and Spin Populations and Energy Gap between the Bands Derived from the HOMO and LUMO of Sc@C_{82} in the Peapods

system	component	$q \text{ (e)}$	$m \text{ (}\mu_B\text{)}$	$\Delta \text{ (eV)}$
$\text{Sc@C}_{82}@(14,7)$	Sc@C_{82}	−0.13	1	0.521
	tube	0.13		
$\text{Sc@C}_{82}@(14,7)^-$	Sc@C_{82}	−0.40	0.60	0.317
	tube	−0.60		
$\text{Sc@C}_{82}@(14,7)^+$	Sc@C_{82}	0.44	0.56	0.293
	tube	0.56		
$\text{Sc@C}_{82}@(11,11)$	Sc@C_{82}	−0.07	1	0.527
	tube	0.07		
$\text{Sc@C}_{82}@(11,11)^-$	Sc@C_{82}	−0.27	0.79	0.414
	tube	−0.73		
$\text{Sc@C}_{82}@(11,11)^+$	Sc@C_{82}	0.05	0.88	0.464
	tube	0.95		

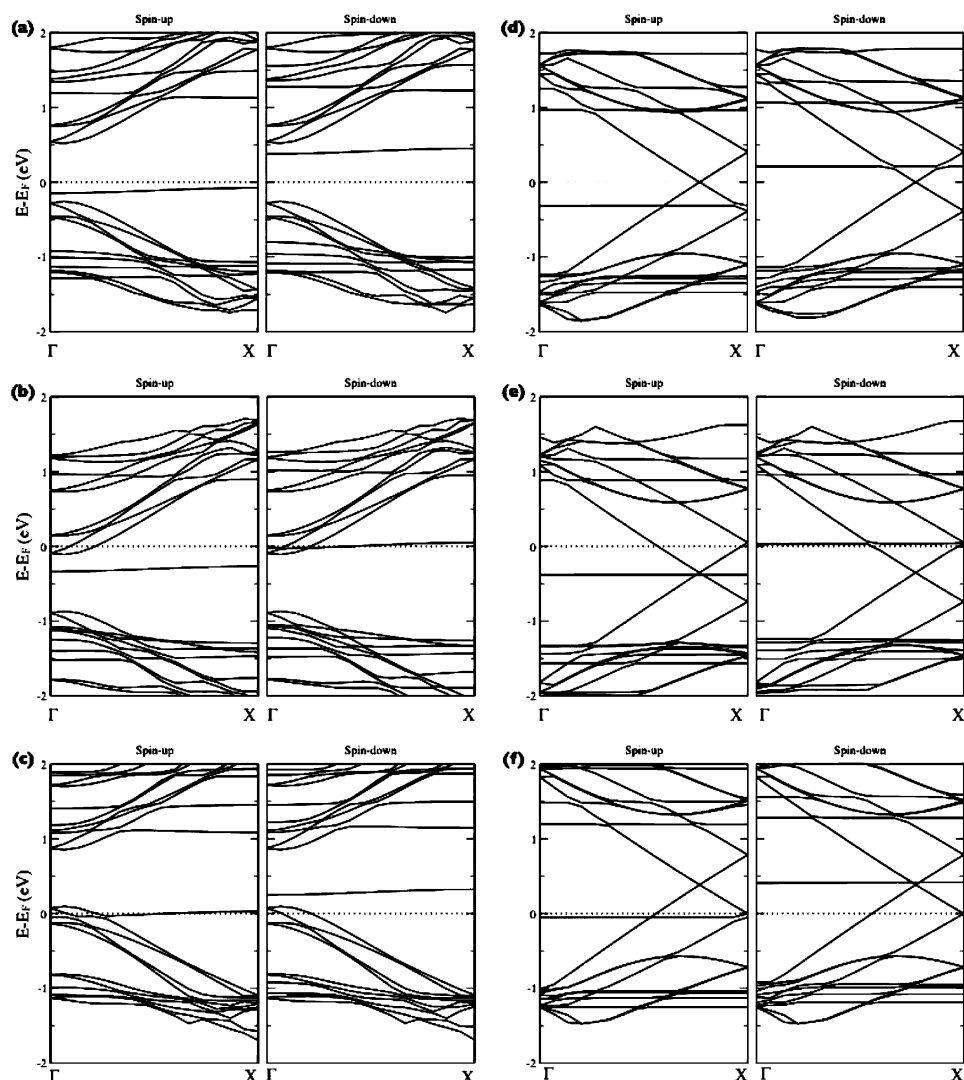


Figure 3. Spin-polarized band structures of (a) $\text{Sc@C}_{82}@(14,7)$ for the FM configuration, (b) $\text{Sc@C}_{82}@(14,7)$ with one extra electron per cell, (c) $\text{Sc@C}_{82}@(14,7)$ with one extra hole per cell, (d) $\text{Sc@C}_{82}@(11,11)$ for the FM configuration, (e) $\text{Sc@C}_{82}@(11,11)$ with one extra electron per cell, and (f) $\text{Sc@C}_{82}@(11,11)$ with one extra hole per cell. E_F is the Fermi energy.

with $\langle n_{\downarrow} \rangle$ unchanged with doping with $\langle n_{\uparrow} \rangle$ increasing from zero.

Figure 4 shows the band structures of $\text{Sc@C}_{82}@(14,7)$ with one electron or hole doped to the unit cell in double cell calculations, that is, an average of $1/2$ electron added or removed per fullerene. These results also show that the upper Hubbard band is pushed up cross-

ing the nanotube conduction bands, giving a band-crossing one-dimensional insulator–metal transition, resembling those in Figure 3b,c. Interestingly, in both cases there are now two conducting channels: a band conductor in the nanotube and a doped Mott-insulator in the fullerene chain. A Mulliken population estimate of the total amount of the doped charge carriers is distributed $\sim 40\%$ on the fullerene chain, and $\sim 60\%$ on the nanotube, consistent with those in $\text{Sc@C}_{82}@(14,7)^-$ and $\text{Sc@C}_{82}@(14,7)^+$. This reveals that the majority of charge always goes to the delocalized nanotube conduction bands under the different doping levels considered. Plotting the wave functions of HOMO-derived bands, we find that the remaining electron or hole on the fullerene chain is equally shared between two fullerenes in the cell, that is, the fullerene bands are derived from dimer bonding orbitals of the pair of fullerenes in the unit cell.

TABLE 3. The Shift of the Spin-up and Spin-down Bands Derived from the HOMO of Sc@C_{82} in Doped Peapods Compared with Undoped Peapods^a

system	ΔE_{\uparrow} (eV)	ΔE_{\downarrow} (eV)
$\text{Sc@C}_{82}@(14,7)^-$	0.438	0.196
$\text{Sc@C}_{82}@(14,7)^+$	−0.245	−0.487
$\text{Sc@C}_{82}@(11,11)^-$	0.289	0.175
$\text{Sc@C}_{82}@(11,11)^+$	−0.117	−0.177

^aThe reference point is the top of nanotube valence bands (in the semiconducting nanotube case) or the anticrossing point of the nanotube linear dispersion conduction and valence bands (in the metallic nanotube case). Positive (negative) values represent the shift upwards (downwards).

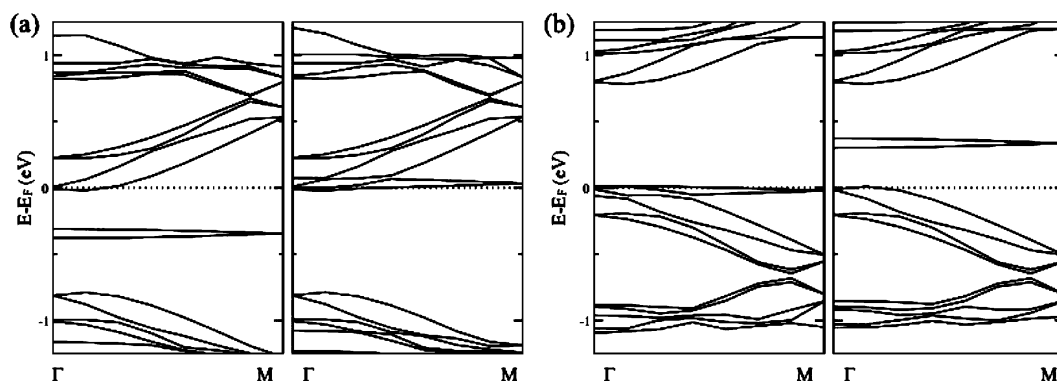


Figure 4. Spin-polarized band structures of $\text{Sc@C}_{82}@(14,7)$ with (a) $1/2$ -electron, or (b) $1/2$ -hole per fullerene; the unit cell contains two fullerenes. Left-(right-)hand side refers to spin-up (-down) electrons. E_F is the Fermi energy.

For the metallic nanotube case, going from Figure 3 panel d to panel e, the spin-up fullerene level has been shifted upward by 0.289 eV relative to the nanotube linear-dispersion conduction and valence bands. In comparison, the spin-down fullerene level has only been shifted upward by 0.175 eV and is pinned at the Fermi energy. For $\text{Sc@C}_{82}@(11,11)$, Δ becomes 0.414 eV with one extra electron per cell. Similar qualitative results have been obtained for the hole case in the metallic tube, as plotted in Figure 3f. Using the same reference point, the spin-up and spin-down fullerene levels have been shifted downward by 0.117 and 0.177 eV compared to Figure 3d, respectively. The band shift in the metallic nanotube cases is less than that in the semiconducting nanotube cases.

The above results show that a rigid band model, assuming that all states are shifted roughly equally by the perturbing potential under n- or p-type doping, is violated for the Sc@C_{82} HOMO-derived states. The observed band crossing insulator–metal transition follows from the changes in the charge (*i.e.*, Coulomb fields) and in the mean magnetic moment (*i.e.*, exchange fields). On one hand, charge distribution is the result of the interplay between additional charge carriers delocalizing in the wide nanotube conduction bands or localizing on the fullerene levels. The former gives lower kinetic energy and Coulomb energy compared to the latter, the majority of the doped electrons or holes going onto the nanotube leaving the minority on the fullerene chain. This redistribution of charge changes the Coulomb fields. On the other hand, the added electron or hole going to the spin-up and -down nanotube conduction bands is paired up, leaving a reduction of the mean magnetic moment, m , on the fullerene chain with a reduction of Δ . The behavior of Δ as a function of m is plotted in Figure 5, showing a significant linear relationship in agreement with eq 5.

It has been shown that a Hubbard–Anderson model with the hybridization parameter $\gamma \approx 5$ meV in the metallic peapod and the Kondo exchange parameter $J_K \approx 0.1$ meV is consistent with DFT results in mean-field for undoped peapods.¹¹ This model is also consistent with

the doped case discussed in this paper and examination of the hybridization gaps and energy shifts show that the systems become pinned in the mixed valence regimes with $\varepsilon_0 + U \approx E_F$ or $E_F \approx \varepsilon_0$ and the hybridization parameter, γ , is in the range of 10–20 meV.

Returning to the questions posed in the introduction, we can now see, for the peapods analyzed in this work, why there is an apparent change in the bandgap of a semiconducting nanotube on insertion of metallofullerenes. For $\text{Sc@C}_{82}@(14,7)$ peapods, the HOMO- and LUMO-derived bands of the fullerene chain lie entirely within the bandgap of the (14,7) nanotube. Furthermore we have shown that these bands are consistent with a half-filled single-band Hubbard model with one-electron (spin) per fullerene cage and intraband excitation energy $\approx U \approx \text{HOMO} - \text{LUMO}$ gap ≈ 0.53 eV. This spin chain was deduced from DFT results of Sc@C_{82} for which intrafullerene charge transfer between Sc and fullerene cage results in a single unpaired electron (spin) delocalized over the fullerene cage for the HOMO state. The intraband band excitation energy of the fullerene chain in the peapod, corresponding to excitation from lower to upper Hubbard bands in spin-polarized DFT, is thus the effective bandgap, significantly less than the nanotube bandgap of ~ 0.82 eV.

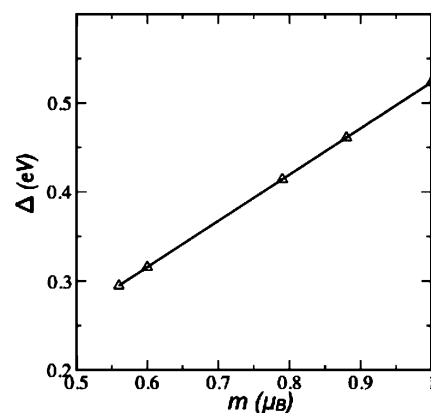


Figure 5. Energy gap between the bands derived from the HOMO and LUMO of Sc@C_{82} in Figure 3, Δ , as a function of the magnetic moment per unit cell, m . Triangles refer to calculated results and are fitted linearly of the form $\Delta = Um$, where $U = 0.530$ eV.

On doping, electrons are either added to, or removed from, the fullerene cages, pinning the Fermi energy to either the upper or lower Hubbard bands. Due to limitations in presently available computing resources, it was only feasible to consider the extreme doping cases of one extra electron or one extra hole per unit cell containing one fullerene. The results show that the occupied fullerene band crosses either the nanotube conduction band (electron doping) or the nanotube valence band (hole doping) when the effective bandgap becomes zero, that is, the nanotube is either n or p doped. The relative shift of the bands is essential for this and was interpreted from a simple electrostatic model. We may now extrapolate these results to smaller doping cases, inaccessible to DFT on currently available resources. As doping is increased from zero, the highest occupied fullerene band will remain within the nanotube bandgap and move toward either the conduction band edge (electrons) or valence band edge (holes). The effective bandgap for the system will then be either the interband excitation energy from fullerene band to nanotube conduction band (electron doping) or interband excitation energy from valence band to fullerene band (hole doping). In both cases the effective bandgap will reduce monotonically to zero with increased doping. The question of the dependence of bandgap on size of fullerenes has not really been addressed in this work since we only consider one kind of fullerene (C_{82}) and nanotubes for which strain due to size mismatch is negligible. For other peapods listed in the introduction, the change in bandgap may be due to other mechanisms, such as strain modulation of the nanotube band edges, as speculated elsewhere.³

CONCLUSION

Under electron or hole doping, the majority of the additional charge always goes on the nanotube with the remainder on the fullerenes in both the semiconducting and metallic nanotube cases considered. This is due to a relative shift of nanotube and fullerene bands, consistent with a simple electrostatic model. There are therefore two conductive pathways in the doped peapods: a one-dimensional doped Mott insulator along the encapsulated fullerene chain and a weakly correlated conductor along the nanotube. The doped peapods are well described by a Hubbard–Anderson model with a linear dependence of the energy gap between the HOMO-derived bands of $Sc@C_{82}$ and the mean magnetic moment. This provides the first step toward an understanding of electrical transport experiments in peapod devices.^{5–10} However, there are several hurdles to overcome before the conductive pathway derived from the fullerene chain can in practice sustain appreciable current. The effective mass of electrons, m^* , associated to the HOMO-derived band of the fullerene chain is rather large ($m^* \approx 1.72m_0$, where m_0 is the free electron mass) and any defect will intro-

duce substantial backscattering. Thus any disorder (e.g., variation of interfullerene spacing or defects in proximity of nanotubes) will give Anderson localization, which will essentially block direct conduction through the fullerene chain, when the length of the peapod exceeds the localization length. Open experimental challenges include the control of interfullerene spacing and purification of nanotubes to increase the localization length. Further investigation needs to take into account charge rearrangement near the contacts and Coulomb blockade effects.²⁰

Acknowledgment. This work is part of QIP IRC. We thank the Materials Chemistry Consortium, EPSRC-GB (Portfolio Grant No. EP/D504872) and MML, Oxford, for providing the computing facilities. L.G. acknowledges support from the Clarendon Fund and St. Anne's College, Oxford. J.H.J. acknowledges support from the UK MOD and Wolfson College, Oxford. G.A.D.B. thanks EPSRC for financial support (GR/S15808/01). We thank J. Warner for discussions.

REFERENCES AND NOTES

- Lee, R. S.; Kim, H. J.; Fischer, J. E.; Thess, A.; Smalley, R. E. Conductivity Enhancement in Single-Walled Carbon Nanotube Bundles Doped with K and Br. *Nature (London)* **1997**, *388*, 255–257.
- Rao, A. M.; Eklund, P. C.; Bandow, S.; Thess, A.; Samlley, R. E. Evidence for Charge Transfer in Doped Carbon Nanotube Bundles from Raman Scattering. *Nature (London)* **1997**, *388*, 257–259.
- Lee, J.; Kim, H.; Kahng, S. J.; Kim, G.; Son, Y. W.; Ihm, J.; Kato, H.; Wang, Z. W.; Okazaki, T.; Shinohara, H.; Kuk, Y. Bandgap Modulation of Carbon Nanotubes by Encapsulated Metallofullerenes. *Nature (London)* **2002**, *415*, 1005–1008.
- Kitaura, R.; Shinohara, H. Endohedral Metallofullerenes and Nano-Peapods. *Jpn. J. Appl. Phys.* **2007**, *46*, 881–891.
- Shimada, T.; Ohno, Y.; Suenaga, K.; Okazaki, T.; Kishimoto, S.; Mizutani, T.; Taniguchi, R.; Kato, H.; Cao, B.; Sugai, T.; Shinohara, H. Tunable Field-Effect Transistor Device with Metallofullerene Nanopeapods. *Jpn. J. Appl. Phys.* **2005**, *44*, 469–472.
- Shimada, T.; Ohno, Y.; Okazaki, T.; Sugai, T.; Suenaga, K.; Kishimoto, S.; Mizutani, T.; Inoue, T.; Taniguchi, R.; Fukui, N.; Okubo, H.; Shinohara, H. Transport Properties of C_{78} , C_{90} , and $Dy@C_{82}$ Fullerenes-Nanopeapods by Field Effect Transistors. *Phys. E* **2004**, *21*, 1089–1092.
- Kobayashi, S.; Mori, S.; Iida, S.; Ando, H.; Takenobu, T.; Taguchi, Y.; Fujiwara, A.; Taninaka, A.; Shinohara, H.; Iwasa, Y. Conductivity and Field Effect Transistor of $La_2@C_{80}$ Metallofullerene. *J. Am. Chem. Soc.* **2003**, *125*, 8116–8117.
- Hiroshiba, N.; Tanigaki, K.; Kumashiro, R.; Ohashi, H.; Wakahara, T.; Akasaka, T. C60 Field Effect Transistor with Electrodes Modified by $La@C_{82}$. *Chem. Phys. Lett.* **2004**, *400*, 235–238.
- Shimada, T.; Okazaki, T.; Taniguchi, R.; Sugai, T.; Shinohara, H.; Suenaga, K.; Ohno, Y.; Mizuno, S.; Kishimoto, S.; Mizutani, T. Ambipolar Field-Effect Transistor Behavior of $Gd@C_{82}$ Metallofullerene Peapods. *Appl. Phys. Lett.* **2002**, *81*, 4067–4069.
- Kurokawa, Y.; Ohno, Y.; Shimada, T.; Ishida, M.; Kishimoto, S.; Okazaki, T.; Shinohara, H.; Mizutani, T. Fabrication and Characterization of Peapod Field-Effect Transistors Using Peapods Synthesized Directly on Si Substrate. *Jpn. J. Appl. Phys.* **2005**, *44*, 1341–1343.
- Ge, L.; Montanari, B.; Jefferson, J. H.; Pettifor, D. G.; Harrison, N. M.; Briggs, G. A. D. Modeling Spin Interactions in Carbon Peapods Using a Hybrid Density Functional Theory. *Phys. Rev. B* **2008**, *77*, 235416.1235416.6.

12. Becke, A. D. Density-Functional Exchange-Energy Approximation with Correct Asymptotic Behavior. *Phys. Rev. A* **1988**, *38*, 3098–3100.
13. Becke, A. D. A New Mixing of Hartree-Fock and Local Density-Functional Theories. *J. Chem. Phys.* **1993**, *98*, 1372–1377.
14. Lee, C.; Yang, W.; Parr, R. G. Development of the Colle-Salvetti Correlation-Energy Formula into a Functional of the Electron Density. *Phys. Rev. B* **1988**, *37*, 785–789.
15. Dovesi, R.; Saunders, V. R.; Roetti, C.; Orlando, R.; Zicovich-Wilson, C. M.; Pascale, F.; Civalieri, B.; Doll, K.; Harrison, N. M.; Bush, I. J.; *et al.* *CRYSTAL06 User's Manual*; University of Torino: Torino, Italy, 2006.
16. Schelegel, H. B. Optimization of Equilibrium Geometries and Transition Structures. *J. Comput. Chem.* **1982**, *3*, 214–218.
17. Mulliken, R. S. Electronic Population Analysis on LCAO-MO Molecular Wave Functions. *J. Chem. Phys.* **1955**, *23*, 1833–1840.
18. Saito, R.; Dresselhaus, G.; Dresselhaus, M. S. *Physical Properties of Carbon Nanotubes*; Imperial College Press: London, 1998; pp 137–159.
19. Morley, G. W.; Herbert, B. J.; Lee, S. M.; Porfyrakis, K.; Dennis, T. J. S.; Nguyen-Manh, D.; Scipioni, R.; van Tol, J.; Hors_eld, A. P.; Ardavan, A.; *et al.* Hyperfine Structure of Sc@C₈₂ from ESR and DFT. *Nanotechnology* **2005**, *16*, 2469–2473.
20. Cantone, A. L.; Buitelaar, M. R.; Smith, C. G.; Anderson, D.; Jones, G. A. C.; Chorley, S. J.; Casiraghi, C.; Lombardo, A.; Ferrari, A. C.; Shinohara, H.; *et al.* Electronic Transport Characterization of Sc@C₈₂ Single-Wall Carbon Nanotube Peapods. *J. Appl. Phys.* **2008**, *104*, 083717-1–083717-7.